Disassembly of Large Composite-Rich Installations

Marco Diani, Nicoletta Picone, Luca Gentilini, Jonas Pagh Jensen, Alessio Angius, and Marcello Colledani

Abstract Considering the demanufacturing of large infrastructures (as wind blades and aircrafts) rich in composite materials, the most impacting step in terms of costs is disassembly. Different routes could be followed for dismantling and transportation and several factors influence the final result (as the technology used, the logistic and the administrative issues). For this reason, it is fundamental to understand which solution has to be followed to reduce the impact of decommissioning on the overall recycling and reusing cost. This work, after the formalization of the different possible disassembly scenarios, proposes a Decision Support System (DSS) for disassembly of large composite-rich installations, that has been designed and implemented for the identification of the most promising disassembly strategy, according to the process costs minimization. The mathematical models constituting the core of this tool are detailed and the DSS is applied to disassembly of onshore wind blades, underling the importance of similar systems to optimize demanufacturing costs.

Keywords Disassembly · Decommissioning · DSS · Cutting · Mechanical treatments · Wind blades · Aircraft

1 Introduction

Disassembly is the most impacting step in demanufacturing, in particular for large infrastructures as wind turbines and aircrafts.

Wind turbines are composed of materials both easily recyclable through well-established practices, as iron and steel, and materials that require innovative solutions,

M. Diani (✉) · L. Gentilini · A. Angius · M. Colledani
Department of Mechanical Engineering, Politecnico Milano, Via La Masa 1, 20156 Milan, Italy
e-mail: marco.diani@polimi.it

N. Picone
STIIMA-CNR, Via Alfonso Corti 12, 20133 Milan, Italy

J. P. Jensen
Siemens Gamesa Renewable Energy A/S, Fiskergade 1-9, 7100 Vejle, Denmark

M. Colledani and S. Turri (eds.), *Systemic Circular Economy Solutions for Fiber Reinforced Composites*, Digital Innovations in Architecture, Engineering and Construction, https://doi.org/10.1007/978-3-031-22352-5_3

as composites. The protection of the environment and the notion of circular economy is gaining increased momentum, which contradicts with the difficulty of recycling the composite parts (mainly blades and nacelle housing) [1].

The composite parts typically consist of fiberglass and a cured resin matrix, namely Glass Fibers Reinforced Plastics (GFRP). The strength of the composites comes from the glass fibers, and therefore, the manufacturers aim to have as much glass in the composite as possible. The normal measurement of the amount of glass in composites is the fiber volume fraction (standard: 55%–60% v/v). The matrix is important for keeping the glass in shape and as a 'carrier' of forces to the glass fibers. These are very strong forces, so the matrix is chemically (i.e. covalently) bonded to the glass fiber, and at the same time the matrix is cross-linked through formation of chemical bonds. This results in an incomparable material when in use, but difficult to recycle.

Due to the fact that recycling of these materials is complex, a wide range of recycling processes has been proposed and tried out—some in commercial settings, others in lab scale attempts [2]. This ranges from architectural reuse of the blade for bike shed, play ground or even walking bridge to more traditional recycling (material recycling), where six main recycling routes, with varying technology readiness levels, are commonly referred to (although the majority of the blades are still reported to end up in landfill) as co-processing in cement kiln, mechanical grinding, pyrolysis, solvolysis, High Voltage Pulse Fragmentation and fluidized bed or gasification. In any case, all these steps are subsequent to the disassembly (or decommissioning) phase.

The decommissioning of a wind farm constitutes the final stage of a project when service life extension or repowering is not a financially feasible practice. It represents the least desirable End-of-Life (EoL) scenario. The main objective of this stage is returning the farm to its original conditions prior to initial deployment. In the decommissioning procedure of a wind farm, all wind tower elements are dismantled (Fig. 1): firstly all blades (GFRP based), nacelle (GFRP based) and the tower (steel based) will be disassembled and hoisted down by crane; then the posterior elements will be disjointed and reduced into smaller pieces suitable for scrap. It is important to underline that the technologies, as well as the qualification and crew for the decommissioning activities used, are comparable to those of the commissioning stage.

Concerning the geographical location, the ideal wind farm installation would have a near constant flow of non-turbulent wind throughout the year, with a minimum likelihood of sudden powerful bursts of wind. An important factor of turbine siting is also access to local demand or transmission capacity. According to these requirements, both onshore and offshore installations would be possible, with limited accessibility in the latter case (only the onshore installations have been considered in FiberEUse).

On the other hand, the handling of EoL aircraft is a relatively young research topic and little knowledge about the aircraft EoL process is available [3]. There is a lack in the norms, since the handling of EoL aircraft has not been legally regulated yet. The common practice for the final disposal of aircraft was to store them besides airports or in deserts around the globe until a few years ago. For decades, thousands of retired aircraft have been stored in so-called aircraft "hot spot" or "graveyards".

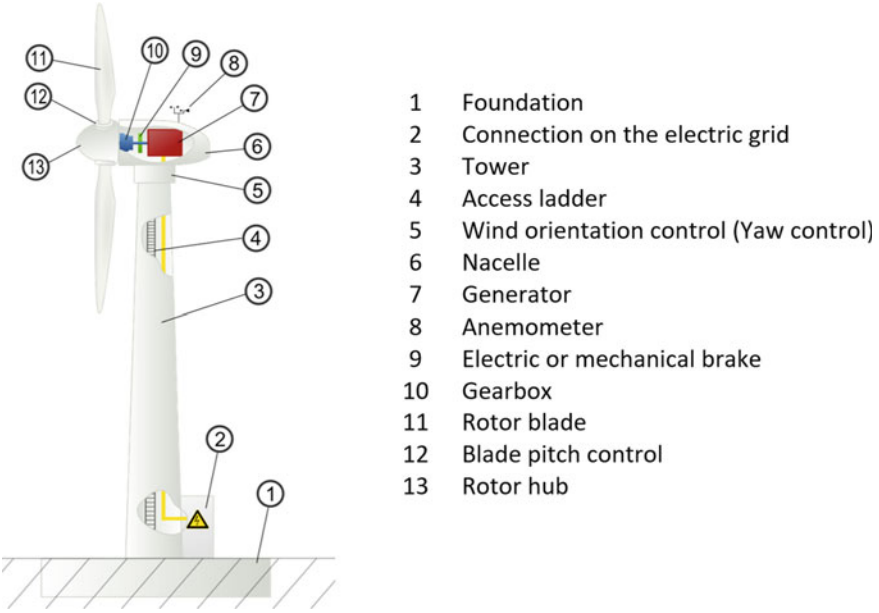

Fig. 1 Wind turbine components

Recently, two largest aircraft manufacturers (Airbus and Boeing) began to develop alternative approaches proposing a three steps process approach of handling EoL aircraft, the so called "3D Approach", based on decommissioning, disassembly and smart dismantling [4]. According to this innovative approach, during the decommissioning process, the aircraft is taken out of service to be inspected, cleaned and decontaminated. Furthermore, all operating liquids are removed and either re-sold for direct re-use or disposed in specific recovery channels. The second step includes the disassembly procedure, defined as a systematic physical separation of a product into its constituent parts, components or other groupings. During this step, knowledge about the specific aircraft type, such as structure, material and part composition needs to be gained in order to define an efficient disassembly planning. The third step takes into consideration recycling and valorization channels, including best practice recommendations and full compliance to applicable regulation. The developed 3D Approach showed the possibility to increase ratio of value creation up to 80–85% (instead of 50–60%), demonstrated a reuse/recycling ratio >70%, showed strong reduction of landfilled waste (<15% instead of 40–45%).

As can be noticed in Fig. 2, composite materials constitute almost 50% of new aircraft design (in this figure a specific example of Boeing 787 is reported), with an average weight saving of 20%. Selecting the optimum material for a specific application meant analyzing every area of the airframe to determine the best material, given the operating environment and loads that a component experiences over the life of the airframe. For example, aluminum is sensitive to tension loads but

handles compression very well. On the other hand, composites are not as efficient in dealing with compression loads but are excellent at handling tension. The expanded use of composites, especially in the highly tension-loaded environment of the fuselage, greatly reduces maintenance due to fatigue when compared with an aluminum structure. This type of analysis has resulted in an increased use of titanium as well. Titanium can withstand comparable loads better than aluminum, has minimal fatigue concerns, and is highly resistant to corrosion. According to the aircraft material composition, almost all the parts could be potentially dismantled for fibers recovery (both CFs and GFs).

From this analysis it is evident the importance of decommissioning and transportation of these parts which are the most impacting factors on the demanufacturing costs. As a consequence, a deep understanding of decommissioning process and an optimization of the demanufacturing process chain is fundamental to achieve a robust circular economy for these products, with a special focus on the cross-sectorial approach. In addition, the large scale dimension of the products requires specific in site disassembly and handling procedures, also enabling possible preliminary on-site treatment (e.g. cutting and mechanical preparation). For this reason a Decision Support System (DSS) for demanufacturing of large infrastructures has been developed and it will be presented in the next Sections.

2 State of the Art

De- and remanufacturing includes the set of technologies and systems, tools and knowledge-based methods to recover and re-use functions and materials from industrial waste and post-consumer high-tech products, to support a sustainable implementation of a new producer-centric Circular Economy paradigm. The goal of de- and remanufacturing systems is inherently different from the goal of a manufacturing system. While manufacturing transforms raw materials into products meeting the customer requirements, de- and remanufacturing transform post-consumer products into valuable materials/new products meeting the customer requirements, for secondary use. However, manufacturing and de- and remanufacturing objectives are clearly not independent. The products that are manufactured and sold to the market today are the products that will be collected and processed in input at the de- and remanufacturing system after the use phase at the customer side. As a consequence, the rapid introduction of new products and the increasing product variety experienced by manufacturers in the last decade is being reflected in the continuous evolution of post-consumer products received in input by de- and remanufacturing systems. This trend represents the main challenge for the development of demanufacturing technological solutions embedding the reconfigurability and adaptability features, efficiently facing the continuous evolution (i.e. complexity) of pre-use products, and the lack of availability and traceability of post-use products information (e.g. design, structure, materials, variability and uncertainty of EoL quality conditions), useful for adapting de- and remanufacturing decisions and operations accordingly.

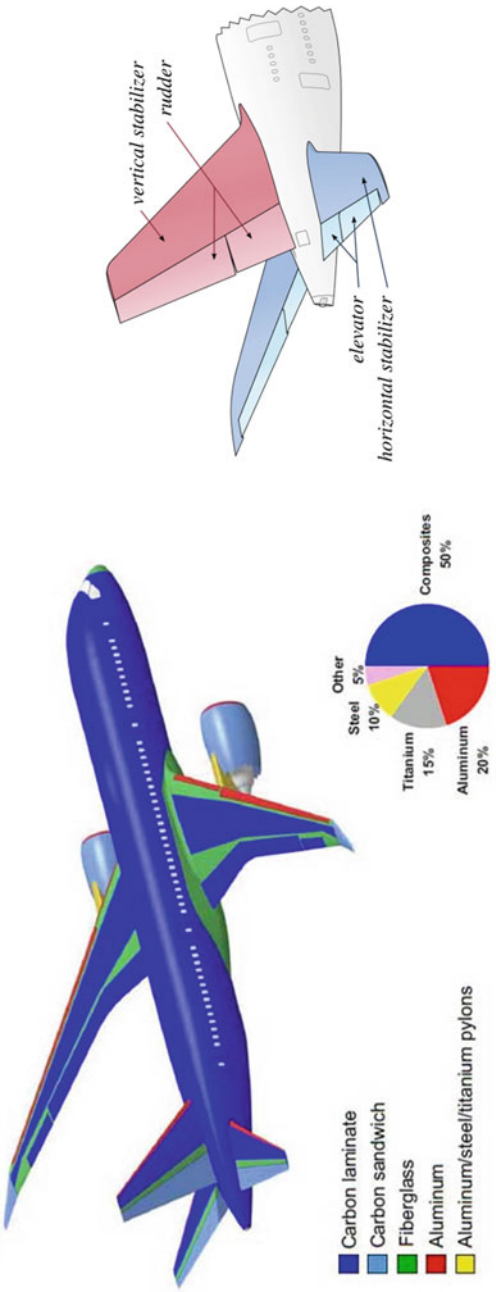

Fig. 2 Composite materials used in Boeing 787 (left); tail composite parts (right)

Therefore, for the full implications of any reuse of recycled Carbon Fibers (rCF) and recycled Glass Fibers (rGF) to be considered, processes, performance, product quality, and markets demand need to be combined to quantify cost benefits of EoL products demanufacturing operations. To this purpose, an in-depth literature review of demanufacturing technologies and processes has been performed.

Concerning the disassembly of EoL products, many studies have been conducted for relatively small products from automotive, electric and electronic sectors (e.g. mechatronic products) as well as for large infrastructure in aeronautic and wind energy sectors [4–6]. In both cases, it has been proved that the disassembly process cannot be simply considered as the reverse of assembly. This is largely due to additional sources of uncertainties, mainly related to the unpredictable characteristics of the returned products (cores) both in terms of quality and quantity [7]. These result from: (i) component defects, (ii) upgrading or downgrading during usage and (iii) damage during the disassembly operation [8]. Therefore, disassembly task planning results to be more complex combinatorial problem than assembly planning. The main aim of disassembly task planning is to find the optimum disassembly path, which is cost effective, improves the value of recovered component and returned material, and respects fixed constraints. Theoretically, the number of possible disassembly sequences increases exponentially with the number of product components and disassembly operations. As a result, finding the optimal solution is an NP-complete optimization problem [8]. In [9] the most effective methodologies and techniques for disassembly task planning are summarized. They include mathematical programming (MP), heuristic methods, to find near-optimal solutions to the disassembly sequencing problem [9], artificial intelligence (AI) methods, e.g. simulated annealing, genetic algorithms (GA), fuzzy sets, neural networks, multi-agent systems, and Bayesian networks, and adaptive planning, for example by Petri Nets, which is used to generate a disassembly sequence with respect to the uncertainties and unexpected circumstances encountered during the disassembly operations.

Concerning the recycling processes, many different technologies have been studied for the last two decades: mechanical processes [10–12], pyrolysis and other thermal processes [13–18], and solvolysis [19, 20]. Some of them, particularly pyrolysis, have even reached an industrial scale, and are commercially exploited: for example, ELG Carbon Fibre Ltd. in United Kingdom use pyrolysis, Adherent Technologies Inc. in USA use a wet chemical breakdown of composite matrix resins to recover fibrous reinforcements and, in France, Innoveox proposes a technology based on supercritical hydrolysis.

According to this review, it is quite clear that currently solutions do exist for the demanufacturing of composite materials. It can be seen in the literature that many different processes and methods have been applied and have shown the feasibility of recovery such materials, some of them being more commercially mature than others. However, industrial applications using recycled fibers or resins are still rare, partly because of a lack of confidence in performance of rGF and rCF, which are considered as of lower quality than virgin ones, but also because rGF and rCF are not completely controlled in terms of length, length distribution, surface quality (adhesion to a new

matrix) or origin (often different grades of fibers are found in a batch of recycled composites coming from different manufacturers) [2].

3 Rationale of the Work

Figure 3 represents an overview of the possible demanufacturing routes for the identified FiberEUse target GFRP/CFRP EoL products/parts, including disassembly, cutting, mechanical and thermal treatments. Literature review on key processes and technologies highlights that many researchers have attempted to study and thus optimize the process parameters in both traditional and non-traditional machining of GFRP and CFRP, to reduce or eliminate the problem of matrix cracking, fiber pull-out, swelling and delamination, thus increasing the surface quality [21]. Failure behaviors do not only arise from the heterogeneous and anisotropic structure, but also from the machining methods and their interactions. These problems are not always significant in the case of demanufacturing of such products: if they should not be remanufactured or reused, the process could be destructive and the potential damages caused during the processing are not relevant. On the other hand, many different techniques for mechanical and thermal treatment, have been studied for the last two decades also reaching high Technology Readiness Level (TRL) and industrial scale applications.

From Fig. 3, the most important processes to be modelled could be derived. In particular, they are: disassembly, cutting, mechanical treatments and thermal treatments. In addition, to develop a robust DSS, it is fundamental to consider also the process boundaries and the macro-constraints as logistic, administrative procedure, operator safety, processing capacity and material requirements. Starting from the analysis of these factors, two different macro-scenarios on the basis of the output material requirements and four different sub-scenarios, according to the possibility to perform a *full in plant treatment*, including exceptional load transport, or a *mixed treatment*, i.e. partially on-site and partially in plant, have been outlined in the next sub-sections and summarized in Fig. 4.

3.1 Selective Cut Macro-Scenario

The application of a selective cut scenario is feasible when the product is characterized by regions with a higher content of fibers. In that case, it could be possible to isolate the fiber rich areas from the rest of the product in order to obtain two output fractions: a high fibers content fraction, to be reused for high level applications, and a low fibers content fraction, to be reused for less demanding applications.

One example is represented by the wind turbine blades. By analyzing their composition, it could be observed that the central longitudinal part (highlighted in red in Fig. 5) shows a higher percentage of GF and/or CF, to withstand the mechanical

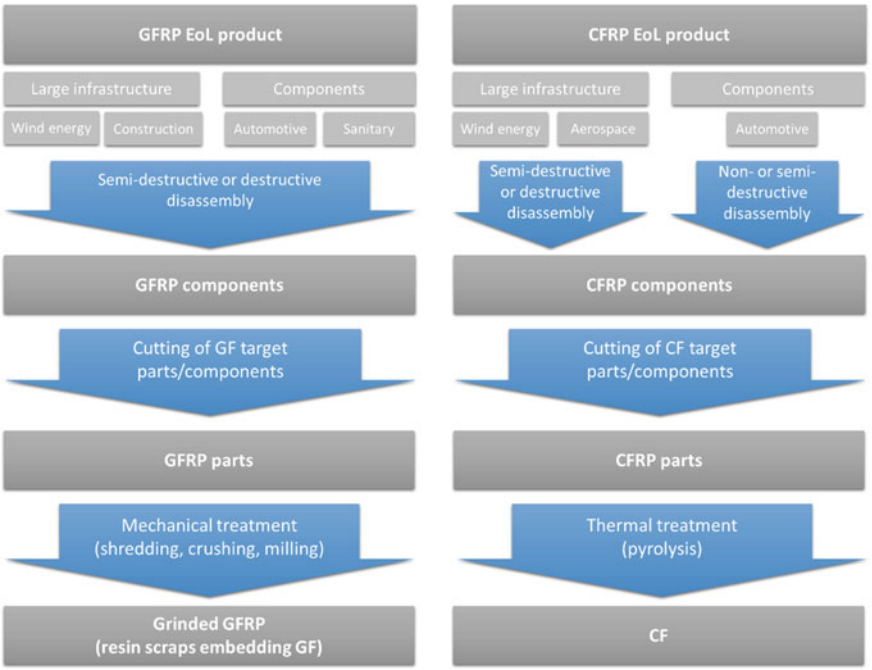

Fig. 3 Demanufacturing routes for the FiberEUse target products/parts

stresses to which they are likely to be subjected. A selective cut following the red dot lines could be a feasible and optimal strategy to enabling two different recycling routes. Following this approach, the material recovered by the central part could be reused for the production of high value products. The two lateral parts, poorer in fiber content, could enter in lower value reuse route.

Another possible approach, is to optimize the disassembly and cutting procedure according to an average fiber content (material requirement), in order to homogenize the output product, both in terms of dimension and fiber concentration. Considering the wind blade structure, the optimal solution (Fig. 6), consists in a longitudinal cut (red dot line) and different transversal cut (green dot lines). In this way, the cut sections have the same percentage of fibers, leading to a homogeneous output.

This selective cut approach is not interesting in the case of parts coming from aeronautic, construction and automotive sectors, which do not present heterogeneity in fibers concentration.

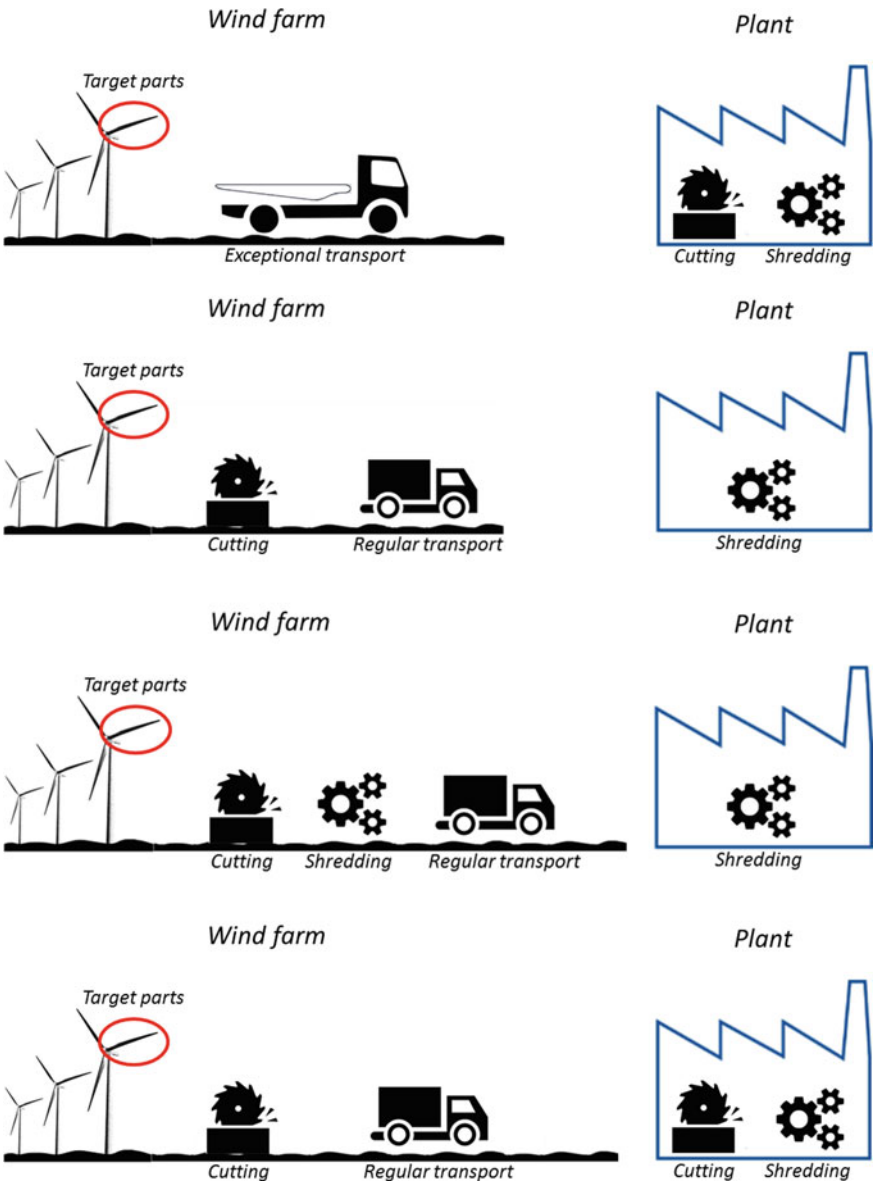

Fig. 4 Considered sub-scenarios. From top to bottom: full in plant treatment; on-site cutting and in plant shredding; on-site cutting, on-site shredding and in plant shredding; on-site cutting, in plant cutting and in plant shredding

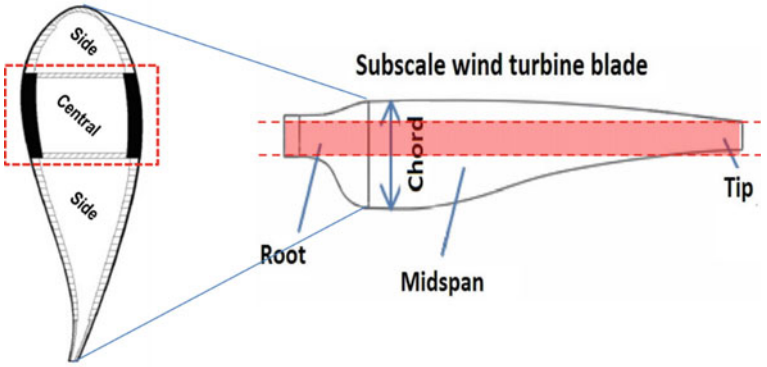

Fig. 5 Top view (right) and cross section (left) of a wind blade. Selective cut scenario for a wind blade providing two different fiber content output fractions

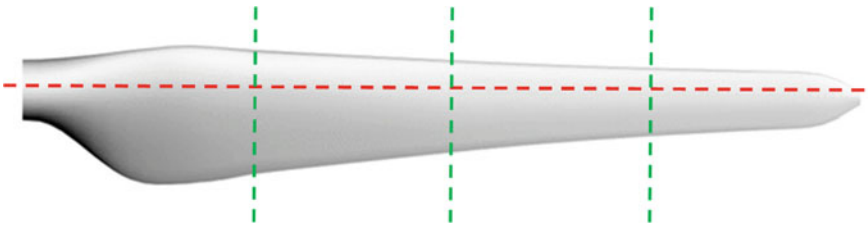

Fig. 6 Selective cut scenario for a wind blade providing average fiber content in output fractions

3.2 Non-selective Cut Macro-Scenario

The application of non-selective cut scenario could be performed for parts characterized by homogeneous fibers content. This is the case of parts coming from aeronautic and construction sectors.

3.3 Mixed Treatment Sub-Scenario

In this sub-scenario different routes are possible: after the preliminary product disassembly, one or more processes could be performed in situ (i.e. cutting and shredding) and one or more in plant (i.e. cutting, shredding, and pyrolysis). In particular, there are five different routes depending on the material under treatment (i.e. GFRP or CFRP). Three of them are related to GFRP products (i.e. GF wind blades and construction components). In this case the identified routes are the following:

- EoL products are cut in situ to increase truck saturation and reach acceptable dimension for further shredding treatment, transported through regular transport and shredded in plant to reach the target output;
- EoL products are cut and shredded in situ to increase truck saturation, transported through regular transport and shredded again in plant to reach the target output dimension;
- EoL products are cut in situ to increase truck saturation, transported through regular transport, cut again in plant to reach acceptable dimension for further shredding treatment and shredded in plant to reach the target output dimension.

The other two routes, related to CFRP and G&CFRP products (i.e. CF wind blades and aircraft parts), are:

– EoL products are cut in situ to increase truck saturation and reach acceptable dimensions for further thermal processing, transported through regular transport and pyrolyzed in plant;
– EoL products are cut in situ to increase truck saturation, transported through regular transport, cut in plant reaching acceptable dimensions for thermal processing and pyrolyzed in plant.

3.4 Full in Plant Treatment Sub-Scenario

In this sub-scenario the disassembled product will be transported as it is to the recycling plant. The most relevant advantages of this solution, in terms of costs, are related to the save of: (i) the administrative costs for in-situ treatment permission (high variable depending on the region of the installation and on the period of the year in which the treatment is performed), (ii) the travel costs for the operators, (iii) the transportation and set-up costs for in-situ treatment machines and (iv) the higher in-situ energy costs (highly variable depending on the geographic area of the installation). On the contrary, this scenario undergoes to higher logistic costs due to the need to perform an exceptional load transport (non-saturated), consequently resulting in a non-optimized transport cost.

The full in plant treatment sub-scenario includes two routes. The one related to GFRP products (i.e. GF wind blades and construction components) is:

– EoL products are dismantled in-situ and transported by using an exceptional load transport to the recycling plant. Here the products are cut to reach acceptable dimension for further shredding treatment.

The route related to CFRP and G&CFRP products (i.e. CF wind blades and aircraft parts) is:

– EoL products are dismantled in-situ and transported by using an exceptional load transport to the recycling plant. Here the products are cut to reach acceptable dimension for further thermal treatment.

4 Methodology

The mathematical model here presented has the scope to create a DSS software tool able to assess the overall treatment costs related to the different scenarios described in Sect. 3. The model is governed at the first hierarchical level by the arbitrary decisions between selective or non-selective cut, and between thermal and mechanical recycling (depending on the type of fibers to be recovered from EoL product). Mathematically:

Variables name	Description	Unit of measure	Variable type
C	Cost of treatment	€	Cumulated
b_{SC}	Boolean: selective cut	Boolean	Input
C_{SC}	Cost of selective cut approach	€	Cumulated
$C_{non\text{-}SC}$	Cost of non-selective cut approach	€	Cumulated

$$C = b_{SC} * C_{SC} + (1 - b_{SC}) * C_{non-SC} \tag{1}$$

Variables name	Description	Unit of measure	Variable type
C_{SC}	Cost of selective cut approach	€	Cumulated
b_{MEC}	Boolean: mechanical recycling	Boolean	Input
$C_{SC\text{-}MEC}$	Cost of mechanical recycling approach	€	Cumulated
$C_{SC\text{-}PYRO}$	Cost of thermal recycling approach	€	Cumulated

$$C_{SC} = b_{MEC} * C_{SC-MEC} + (1 - b_{MEC}) * C_{SC-PYRO} \tag{2}$$

Variables name	Description	Unit of measure	Variable type
$C_{non\text{-}SC}$	Cost of non-selective cut approach	€	Cumulated
b_{MEC}	Boolean: mechanical recycling	Boolean	Input
$C_{non\text{-}SC\text{-}MEC}$	Cost of mechanical recycling approach	€	Cumulated
$C_{non\text{-}SC\text{-}PYRO}$	Cost of thermal recycling approach	€	Cumulated

$$C_{non-SC} = b_{MEC} * C_{non-SC-MEC} + (1 - b_{MEC}) * C_{non-SC-PYRO} \tag{3}$$

Resulting in a cost for transportation C_{TR} equal to:

$$C_{TR} = b_{SC} * \left[b_{MEC} * C_{SC-MEC} + (1 - b_{MEC}) * C_{SC-PYRO}\right] + (1 - b_{SC}) * \left[b_{MEC} * C_{non-SC-MEC} + (1 - b_{MEC}) * C_{non-SC-PYRO}\right] \quad (4)$$

An application example about the non-selective cut scenario for GFRP product is modelled in the following section. In the case of different input flows, the core of the mathematical model remains the same and it's scalable to the other macro- and sub-scenarios, for each of which specific objective function should be derived. The main differences to be implemented for the other cases are here reported:

- In case of selective cut strategy, a first stage selective cut has to be added both for GFRP and CFRP products. The cut can be performed either on-site or in plant. Please notice that selective cut on-site enables all the other on-site treatments. For the selective cut contour, resulting in the cutting length, the cutting optimization algorithm can be exploited. Once performed the selective cut, the main optimization model can be applied separately to the N shapes resulting from the first cut.
- In case of CFRP products, shredding costs have to be properly substituted by pyrolysis costs. On-site coarse shredding to enable transport saturation through size reduction is not a viable option in case of thermal recycling.

4.1 Application Example: Non-Selective Cut Scenario for GFRP Products

According to the previous analysis, the model has the objective to select the cheapest option among the following possible routes:

- Route 1: EoL products are cut in situ to increase truck saturation and reach acceptable dimension for further shredding treatment, transported through regular transport and shredded in plant to reach the target output dimension;
- Route 2: EoL products are cut and shredded in situ to increase truck saturation, transported through regular transport and shredded again in plant to reach the target output dimension;
- Route 3: EoL products are cut in situ to increase truck saturation, transported through regular transport, cut again in plant to reach acceptable dimension for further shredding treatment and shredded in plant to reach the target output dimension.
- Route 4: EoL products are dismantled in-situ and transported by using an exceptional load transport to the recycling plant. Here the products are cut to reach acceptable dimension for further shredding treatment.

The objective function behind this model is reported in the following:

$$C_{non-SC-MEC} = min \sum_{i=1}^{4} b_{MEC-i} * C_{non-SC-MEC-i} \quad (5)$$

Variables name	Description	Unit of measure	Variable type
$C_{non\text{-}SC\text{-}MEC}$	Cost of mechanical recycling approach	€	Cumulated
b_{MEC-i}	Boolean: route *i*	Boolean	Decision
$C_{non\text{-}SC\text{-}MEC-i}$	Cost of route *i*	€	Cumulated

Constrained by:

$$\sum_{i=1}^{4} b_{MEC-i} = 1 \quad (6)$$

The objective function has been derived for the four possible routes. For space reasons, the procedure will be shown only for one route.

Route 1: full on-site cutting and full in plant shredding

Variables name	Description	Unit of measure	Variable type
$C_{non\text{-}SC\text{-}MEC-1}$	Cost of route 1	€	Cumulated
$C_{OS\text{-}cutS-1}$	Cost of on-site cutting	€	Cumulated
C_{TR-1}	Ordinary transport cost	€	Cumulated
$C_{IP\text{-}shred-1}$	Cost of in plant shredding	€	Cumulated

$$C_{non-SC-MEC-1} = C_{OS-cut-1} + C_{IP-shred-1} + C_{TR-1} \quad (7)$$

Variables name	Description	Unit of measure	Variable type
$C_{OS\text{-}cut-1}$	Cost of on-site cutting	€	Cumulated
$C_{OS\text{-}cut\text{-}admin}$	On-site cutting administrative cost	€	Fixed
$C_{OS\text{-}cut\text{-}setup}$	On-site cutting set-up cost	€	Fixed
N	Number of blades	Pure, int	Input
$C_{OS\text{-}op}$	On-site cost of operator	€/h	Fixed
$C_{OS\text{-}cut}$	Energy and wear cutting-related costs	€/h	Fixed
L_1	Total cutting length	m	Algorithm

(continued)

(continued)

Variables name	Description	Unit of measure	Variable type
Th	Average thickness of the blade	m	Input
s_c	Cutting speed	m^2/h	Fixed

$$C_{OS-cut-1} = C_{OS-cut-admin} + C_{OS-cut-steup} + N * (C_{OS-op} + C_{cut}) * \frac{L_1 * 2 * th}{s_c} \quad (8)$$

The total cutting length is calculated by a dedicated developed algorithm presented in Sect. 4.2. The optimization algorithm works with a one-sided 2D image. For this reason the real cutting length is the double of the one received from the algorithm.

Variables name	Description	Unit of measure	Variable type
$C_{IP\text{-}shred-1}$	Cost of in plant shredding	€	Cumulated
$C_{IP\text{-}shred\text{-}setup}$	In plant shredding set-up cost	€	Fixed
N	Number of blades	Pure, int	Input
C_{shred}	Energy and wear shredding-related costs	€/h	Fixed
A	Surface of the blade (one side only)	m^2	Input
Th	Average thickness of the blade	m	Input
TH_{sh-1}	Shredder throughput	m^3/h	Algorithm

$$C_{IP-shred-1} = C_{IP-shred-setup} + N * C_{shred} * \frac{2 * A * th}{TH_{sh-1}} \quad (9)$$

The shredding throughput depends on the target output particle size, which determines the shredder grate size. Shredding throughput modelling breakdown is modeled in a dedicated algorithm and here is just summarized.

Variables name	Description	Unit of measure	Variable type
TH_{sh-1}	Shredder throughput	m^3/h	Algorithm
K_{sh}	Technology dependent constant	m^2/h	Fixed
d_{grate}	Grate size	mm	Input

$$TH_{sh-1} = K_{sh} * \frac{d_{grate}}{1000\,\text{mm/m}} \quad (10)$$

Variables name	Description	Unit of measure	Variable type
C_{TR-1}	Ordinary transport cost	€	Cumulated
N_{TR-1}	Number of transports needed	Pure, int	Cumulated
$C_{TR\text{-}fixed}$	Transportation fixed cost	€	Fixed
$C_{TR\text{-}km}$	Transportation cost-per-kilometer	€ / km	Fixed
$D_{plant\text{-}farm}$	Wind farm—recycling plant distance	km	Input
V_{real-1}	Gross volume of blade pieces	m^3	Algorithm
$V_{max\text{-}truck}$	Maximum volume of a container	m^3	Fixed

$$C_{TR-1} = N_{TR-1} * \left[C_{TR-fixed} + C_{TR-km} * D_{plant-farm}\right] \tag{11}$$

$$N_{TR-1} = int^{+}\left\{\frac{V_{real-1}}{V_{max-truck}}\right\} \tag{12}$$

The gross volume to be transported is calculated by a dedicated algorithm and here, only the final mathematical formula is reported.

Variables name	Description	Unit of measure	Variable type
V_{real-1}	Real volume to be transported	m^3	Algorithm
V_{net}	Net GFRP volume	m^3	Cumulated
n_{cuts}	Number of cuts to be performed on-site	Pure number	Decision
A	Surface of the blade (one side only)	m^2	Input
th	Average thickness of the blade	m	Input

$$V_{real-1} = \left[\frac{n_{cuts}+4}{n_{cuts}+1} + \frac{1}{\sqrt[3]{n_{cuts}+3}}\right] * V_{net} \tag{13}$$

where:

$$V_{net} = 2 * A * th \tag{14}$$

4.2 Cutting Process Modelling

Cutting length and number of cuts. A dedicated optimization algorithm (*Cutting Optimizator CO*) has been developed to evaluate a case-by-case optimal cutting

strategy. The algorithm is able to treat a general digital image, here representing the wind blade, extrapolate the contour, and investigate an optimal cutting strategy to satisfy the model limitations (as pieces final size and concentration) maximizing or minimizing a set of pre-defined variables, as total cutting length, homogeneity within pieces, etc.

The *Cutting Optimizator* (CO) has been implemented in Python 3.0 and consists in a set of classes and methods that allows the user to find a sub-optimal cutting strategy for a surface having general shape. The CO offers methods to retrieve the contour of a surface and define lines (cuts) on it in order to split the surface and analyze the properties of the resulting parts. The CO provides also the possibility to couple the surface with a function that specify the concentration of material for each point contained in the surface.

The core of CO is a method, called "*ComputeCutting*" that takes in input:

- the set of points describing the contour of the surface to be cut,
- the maximal length and width of the parts that arise from the cutting,
- the maximal concentration of material of the parts that arise from the cutting.
- a general user-defined function **f(−)**

The output is a set of cuts that optimize the splitting of the surface according to **f**. The function **f** has been left general in such a way that the user can specify his own criteria. However, the input parameters of **f** are fixed. In particular, the function receives:

- A surface to be split,
- Two points, namely **a** and **b**, that define the line of the cut,
- The description of the current best cut (two points, score value and the two parts that are generated by the cut),
- Three possible weights that can be used for general purposes.

Function **f** returns the best cut between the cut defined by **a** and **b**, and the best cut.

The method "*ComputeCutting*" works on any kind of shape as long as its contour is specified as an array of x–y coordinates. Despite this, the CO offers a method that retrieves the set of coordinates from a digital image. This functionality has been included to avoid the manual generation of the shape of the surface under investigation.

The shape recognition is implemented by using the OpenCV library [22].

The optimization method. The optimization method implements a "*divide et impera*" strategy. The starting point is the original surface. The method finds the best cut to split the surface in two by using **f** to compare all the possible cuts. The best cut is used to generate two smaller parts. These two parts are stored and split in two parts each by using the same strategy that has been used for the original surface. The method cycles until all the parts satisfy the dimension and concentration criteria. Each cycle works with parts that are smaller than the predecessor.

Function f. At this moment, the function **f** is defined in such a way that it considers the minimal difference between:

- the length and the width of the projection of each part on a rectangle (denoted with **d**)
- the (approximated) concentration of each part (denoted with **c**)

and the length of the cut (denoted with **l**). The objective function is the weighted sum of these three measures. The best cut is the one able to minimize the sum. The measure **d**, **c** and **l** are normalized in such a way that no measure can dominate the others. Furthermore, each measure is associated with a weight that allows the user to increase the impact of one on the others.

On-site optimal cutting length and number of cuts. The cutting optimization algorithm provides a set of cuts with an inner hierarchy. There is a first cut, a second cut, a third and so on. Each of these cuts is associated with its own length. In the table below an example of a set of cuts provided by the algorithm, each one with its cutting length. The total cutting length exploited in all the other scenarios (full on-site cutting or full in plant cutting) is the sum of the single lengths.

Cut (#)	Length (m)
1	1.3
2	0.9
3	1
4	0.8
5	0.5
6	0.6
7	0.4
L, total cutting length (m)	5.5

The overall optimization model takes this cutting hierarchy and analyzed for each cutting level the associated on-site treatment costs and transportation cost, under the main assumptions that the more on-site cuts the more transport saturation.

For example:

Cut (#)	Length (m)	Number of on-site cuts	L*	L − L*
1	1.3	1	1.3	4.2
2	0.9	2	2.2	3.3
3	1	3	3.2	2.3
4	0.8	4	4	1.5
5	0.5	5	4.5	1
6	0.6	6	5.1	0.4
7	0.4	7	5.5	0

(continued)

(continued)

Cut (#)	Length (m)	Number of on-site cuts	L*	L − L*
L, total cutting length (m)	5.5			

For each of the seven hierarchy levels:

– The number of on-site cuts is exploited by the saturation algorithm to estimate the transport saturation and so the transportation costs.
– The on-site cutting length L* is exploited to calculate the costs of on-site cutting.
– The in plant cutting length L − L* is exploited to calculate the costs of in plant cutting.

Having these data, the main model is able to calculate the overall treatment costs associated to the on-site cutting for each hierarchy level and highlight the best solution.

5 Numerical Results

The development of the DSS as an ICT solution to drive the operator in the selection of the best demanufacturing route for each specific product under treatment has been based on an approach including the following main phases:

- identification of target composite products/parts in the four FiberEUse industrial sectors (i.e. wind energy, construction, aerospace and automotive);
- definition of a set of potentially significant quality characteristics to be evaluated before disassembly (e.g. type of connection, the critical issues related to the current disassembly procedures, disassembly technologies, as well as the logistics requirements);
- collection and analysis of requirements for each input product;
- clustering of the collected information in two macro-categories: products integrated in large infrastructures (i.e. wind blades, aircraft parts and construction components) and components from automotive sector (i.e. seat structure, rear panel, front-end, gear tunnel, leaf spring, monocoque, roof stiffener, roof bow, resonator, seat shell);
- definition of the recycling oriented integrated disassembly and transport problem;
- definition of the disassembly planning problem following two approaches, one for large infrastructures (innovative mathematical model) and one for components (common disassembly planning algorithms);
- definition of the DSS features for the identification of the most promising disassembly strategy for large infrastructures, according to the process costs minimization;
- implementation and validation of the DSS.

A model, implemented in Python 3.0 and MatLab, was developed to identify the most promising disassembly strategy in terms of costs minimization. The basic equations behind this model are addressed to analyze the identified scenarios and solve the related recycling oriented integrated disassembly and transport problem, in order to optimize the disassembly planning problem.

The main objective function is reported in the following:

$$minC = C_{OS-TREATMENTS} + C_{TRANSPORT} + C_{IP-TREATMENT} \quad (15)$$

$$minC = C_{OS-cut} + C_{OS-sh} + C_{TRANSPORT} + C_{IP-cut} + C_{IP-sh} + C_{IP-th} \quad (16)$$

Each term of the objective function is then related to specific variables described in the following:

- C_{OS-cut}. The cost for on-site cutting treatment depends on the: (i) cutting technology (feed rate, speed), (ii) energy consumption and tool wear, (iii) personnel costs, and (iv) set-up costs,
- C_{OS-sh}. The cost for on-site shredding treatment depends on the: (i) shredding technology (feeder dimension, feed rate, speed), (ii) energy consumption and tool wear, (iii) personnel costs, (iv) set-up costs and (v) output particles size (grate dimension),
- C_{IP-cut}. The cost for in plant cutting treatment depends on the: (i) cutting technology (feed rate, speed), (ii) energy consumption and tool wear, and (iii) personnel costs,
- C_{IP-sh}. The cost for in plant shredding treatment depends on the: (i) shredding technology (feeder dimension, feed rate, speed), (ii) energy consumption and tool wear, (iii) personnel costs, and (iv) output particles size (grate dimension),
- C_{IP-th}. The cost for thermal treatment depends on the: (i) technology (capacity), (ii) energy consumption, (iii) personnel costs, and (iv) residence time.

In order to provide a software tool that could be used in different disassembly problem, a specific software module has been designed and implemented. This software takes in input information about the product, technologies and logistic and administrative aspects (Table 1). Starting from these data, the tool runs the optimization and provides in output to the user the optimized disassembly strategy to isolate the target composite-made parts/components.

Preliminary validation tests have been performed for the demonstration of the efficiency of the developed DSS software tool. In the demonstration phase, the values of the input model variables have been provided by the FiberEUse industrial partners (i.e. material providers, material processors or end-users, logistic operators) directly involved at different levels of the value-chain.

Table 1 Input model variables

Category	Name	Description	Unit of measure
Product	N	Number	–
	D_1	Lenght	m
	D_2	Width	m
	D_3	Height	m
	th	Thickness	m
Selective disassembly	SD	Y/N	–
Personnel cost	$C_{OS\text{-}OP}$	On-site operator costs	€/h
	$C_{IP\text{-}OP}$	In plant operator costs	€/h
On-site cutting techonology	$C_{OS\text{-}CUT\text{-}E}$	Energy consumption and tool wear	€/h
	$s_{OS\text{-}CUT}$	Cutting speed	m min^{-1}
	$fr_{OS\text{-}CUT}$	Feed rate	m min^{-1}
	$C_{OS\text{-}CUT\text{-}SET}$	Set-up costs	€
In plant cutting techonology	$C_{IP\text{-}CUT\text{-}E}$	Energy consumption and tool wear	€/h
	$s_{IP\text{-}CUT}$	Cutting speed	m min^{-1}
	$fr_{IP\text{-}CUT}$	Feed rate	m min^{-1}
	$C_{IP\text{-}CUT\text{-}SET}$	Set-up costs	€
On-site shredding technologies	$sh_{OS\text{-}l}$	Feeder lenght	m
	$sh_{OS\text{-}w}$	Feeder width	m
	$C_{OS\text{-}SH}$	Energy consumption and tool wear	€/h
	$s_{OS\text{-}SH}$	Feed rate (model)	m^3/h
	$d_{OS\text{-}SH}$	Output particles dimension	mm
	$C_{OS\text{-}SH\text{-}SET}$	Set-up costs	€
	$sat_{OS\text{-}SH}$	Saturation (model)	–
	$su_{OS\text{-}SH}$	Downstream shred speed-up (model)	–
In plant shredding technologies	$sh_{IP\text{-}l}$	Feeder lenght	m
	$sh_{IP\text{-}w}$	Feeder width	m
	$C_{IP\text{-}SH}$	Energy consumption and tool wear	€/h
	$s_{IP\text{-}SH}$	Feed rate (model)	m^3/h
	$d_{IP\text{-}SH}$	Output particles dimension	mm
	$C_{IP\text{-}SH\text{-}SET}$	Set-up costs	€
In plant thermal technologies	$th_{IP\text{-}l}$	Feeder lenght	m
	$th_{IP\text{-}w}$	Feeder width	m

(continued)

Table 1 (continued)

Category	Name	Description	Unit of measure
	$C_{IP\text{-}TH}$	Energy consumption	kw/h
	$s_{IP\text{-}TH}$	Capacity	m^3/h
Logistic	$C_{TR\text{-}OVS}$	Exceptional load transport (included personnel)	€/km
	$C_{TR\text{-}REG}$	Non-exceptional load transport (included personnel)	€/km
	$C_{TR\text{-}FEE}$	Fee exceptional load	€
	$C_{TR\text{-}ML}$	Max load	m^3
	d_{TR}	Distance between installation and plant	km
Administrative	$C_{PER\text{-}OS\text{-}CUT}$	Permission on site cut	€
	$C_{PER\text{-}OS\text{-}SH}$	Permission on site shredding	€

The software tool has been validated according to the non-selective cut scenario for GFRP wind blades. Some of the input data of the demonstration test are reported in the following:

- product: GF wind blade;
- number of products: 18 wind blades (wind turbines: 6);
- strategy: non-selective cutting;
- site-plant distance: 500 km;
- target output particles dimension: 6 mm.

The model has the objective to select the cheapest option among the following possible routes:

- Route 1: GF wind blades are cut in situ to increase truck saturation and reach acceptable dimension for further shredding treatment, transported through regular transport and shredded in plant to reach the target output dimension;
- Route 2: GF wind blades are cut and shredded in situ to increase truck saturation, transported through regular transport and shredded again in plant to reach the target output dimension;
- Route 3: GF wind blades are cut in situ to increase truck saturation, transported through regular transport, cut again in plant to reach acceptable dimension for further shredding treatment and shredded in plant to reach the target output dimension.
- Route 4: GF wind blades are dismantled in-situ and transported by using an exceptional load transport to the recycling plant. Here the products are cut to reach acceptable dimension for further shredding treatment.

The results of validation are reported in Table 2.
According to the input values, the optimal disassembly scenario is Route 3.

Table 2 Demonstration test results: non-selective cut scenario for GFRP wind blades

Cost for Route 1 (€)	Cost for Route 2 (€)	Cost for Route 3 (€)	Cost for Route 4 (€)
79.28992	81.90088	78.67105	91.94732

6 Conclusions

In this Chapter, effective and efficient solutions and approaches for the disassembly of EoL composite products coming from different sectors have been analyzed in depth, in order to derive the most promising disassembly strategy to isolate the target composite-made parts/components.

Different macro- and sub-scenarios have been analyzed and specific mathematical models for large infrastructures have been developed and proposed.

Finally, the developed models have been validated and a specific software tool, based on a DSS approach, has been designed and implemented for the automatic identification of the most promising disassembly strategy. This software takes in input information about the characteristics of EoL product, the key processes and technologies, logistic aspects, the required target output product (both in terms of dimension and fibers content) and provides to the user the cutting path (if needed) and the optimal disassembly scenario, according to the process costs minimization. Similar conclusions can be outlined for the disassembly of EoL airplanes, considering the different technologies to treat CFRP, for which the mixed treatment is the best solution.

References

1. MacArthur, E., et al.: Towards the circular economy. J. Ind. Ecol. **2**, 23–44 (2013)
2. Oliveaux, G., Dandy, L., Leeke, G.: Current status of recycling of fibre reinforced polymers: review of technologies, reuse and resulting properties. Progress in Materials Science 61–99 (2015)
3. Perry, J.: Sky-high potential for aircraft recycling. Aircraft Maintenance, pp. 2–5 (March 2012)
4. Ribeiro, J.S., de Oliveira Gomes, J.: Proposed framework for end-of-life aircraft recycling. Procedia CIRP **26**, 311–316 (2015)
5. Dayi, O., Afshar, A.: A lean based process planning for aircraft disassembly. IFAC-PapersOnLine **49**(2), 054–059 (2016)
6. Martinez Luengo, M., Kolios, A.: Failure mode identification and end of life scenarios of offshore wind turbines: a review. Energies **8**(8), 8339–8354 (2015)
7. Vongbunyong, S., Chen, H.W.: Disassembly automation, pp. 25–54. Springer, Cham (2015)
8. Gungor, A., Gupta, S.M.: An evaluation methodology for disassembly processes. Comput Ind Eng **33**(1–2), 329–332 (1997)
9. Lambert, A.J.D.: Disassembly sequencing: a survey. Int. J. Prod. Res. **41**(16), 3721–3759 (2003)
10. Pickering, S.J.: Recycling technologies for thermoset composite materials—current status. Compos. A **37**, 1206–1215 (2006)

11. Schinner, G., Brandt, J., Richter, H.: Recycling carbon-fiber-reinforced thermoplastic composites. J Thermoplast Compos Mater **9**, 239–245 (1996)
12. Kouparitsas, C.E., Kartali, C.N., Varelidis, P.C., Tsenoglou, C.J., Papaspyrides, C.D.: Recycling of the fibrous fraction of reinforced thermoset composites. Polym Compos **23**, 682–689 (2002)
13. Torres, A., de Marco, I., Caballero, B.M., Laresgoiti, M.F., Legarreta, J.A., Cabrero, M.A.: Recycling by pyrolysis of thermoset composites: characteristics of the liquid and gases fuels obtained. Fuel **79**, 897–902 (2000)
14. Cunliffe, A.M., Williams, P.T.: Characterisation of products from the recycling of glass fibre reinforced polyester waste by pyrolysis. Fuel **82**, 2223–2230 (2003)
15. Feih, S., Boiocchi, E., Mathys, G., Mathys, Z., Gibson, A.G., Mouritz, A.P.: Mechanical properties of thermally-treated and recycled glass fibres. Compos. B **42**, 350–358 (2011)
16. Gosau, J.M., Tyler, F.W., Allred, R.E.: Carbon fiber reclamation from state-of-art 2nd generation aircraft composites. In: Proceedings of the international SAMPE symposium and exhibition. Baltimore, MD, USA (2009)
17. Åkesson, D., Foltynowicz, Z., Christéen, J., Skrifvars, M.: Microwave pyrolysis as a method of recycling glass fibre from used blades of wind turbines. J Reinf Plast Compos **31**, 1136–1142 (2012)
18. López, F.A., Rodríguez, O., Alguacil, F.J., García-Díaz, I., Centeno, T.A., García-Fierro, J.: Recovery of carbon fibres by the thermolysis and gasification of waste prepeg. J. Anal. Appl. Pyrol. **104**, 675–683 (2013)
19. Iwaya, T., Tokuno, S., Sasaki, M., Goto, M., Shibata, K.: Recycling of fiber reinforced plastics using depolymerization by solvothermal reaction with catalyst. J. Mater. Sci. **43**, 2452–2456 (2008)
20. Pinero-Hernanz, R., Dodds, C., Hyde, J., Garcia-Serna, J., Poliakoff, M., Lester, E.: Chemical recycling of carbon fibre reinforced composites in nearcritical and supercritical water. Compos. A **39**, 454–461 (2008)
21. Chandramohan, D., Murali, B.: Machining of composites—a review. Academic Journal of Manufacturing Engineering **12**(3), 67–71 (2014)
22. Open CV Homepage. https://opencv.org/. Last accessed 15 March 2021